

# INTERNATIONAL SOCIETY FOR SOIL MECHANICS AND GEOTECHNICAL ENGINEERING



*This paper was downloaded from the Online Library of the International Society for Soil Mechanics and Geotechnical Engineering (ISSMGE). The library is available here:*

<https://www.issmge.org/publications/online-library>

*This is an open-access database that archives thousands of papers published under the Auspices of the ISSMGE and maintained by the Innovation and Development Committee of ISSMGE.*

# DYNAMIC CYCLIC STRAIN TESTS ON A CLAY

## ESSAIS DYNAMIQUES D'ARGILE A VITESSE DE DEFORMATION CONTROLEE

P.W. TAYLOR, B.Sc., B.E.

University of Auckland, New Zealand

D.R. BACCHUS, B.E., Engineer

Tonkin & Taylor, Auckland, New Zealand

### SYNOPSIS

Dynamic triaxial tests are described in which one hundred sinusoidal strain-controlled cycles were applied to artificially-prepared saturated clay samples. The significant effect on normally consolidated clays was to reduce the mean effective stress at a rate dependent on the applied strain amplitude. Peak shear stress and damping energy were found to be related to the mean effective stress. The stress-strain relationship showed a degradation to an 'S'-shaped loop. The changes in 'elastic' and plastic properties of the clay are attributed to the development of a more dispersed structure.

### INTRODUCTION

When a clay is subjected to repeated strain cycles it undergoes irreversible structural changes and a degradation in elastic and plastic properties (i. e. stiffness and damping). The apparatus and experimental procedure described herein were designed to study the changes in mean effective stress with the application of a number of strain cycles (of various magnitudes) to initially undisturbed specimens of clay. The pore-pressure measuring system was developed which incorporated a transducer with very low volume change characteristics, giving rapid response. During strain-controlled tests, degradation results in a reduction of energy input per cycle whereas with stress-control the reverse is the case.

### THE APPARATUS

The apparatus used for the testing program consisted essentially of a triaxial cell, an arrangement for applying a cyclic strain to the soil, and an electronic recording system. The mechanical apparatus is shown diagrammatically in Figure 1.

The triaxial cell was designed to accommodate 3" diameter, 6" long specimens. Non-tilting, polished chrome end platens were covered by a .012" thick rubber membrane lubricated with silicone grease. As excess grease was extruded during consolidation, the thickness of the grease film and hence the viscous resistance of the system was determined by the maximum consolidation pressure.

The drainage system consisted of twelve 3/8" wide filter paper side-drains and a 3/4" diameter porous disc in contact with the base of the specimen.

A vertical sinusoidal strain ranging in amplitude from 0.01% to 10% could be applied to the specimens by a motor-driven eccentric controlled by an electric clutch and brake. The starting position of the eccentric was set so that equal strain was applied in both extension and compression.

Axial load and strain were recorded by means of electrical transducers incorporating linear differential transformers. The load transducer was embodied in the load rod itself inside the cell so that measurement did not include the friction between rod and bushing. Strain was measured outside the cell. Pore-pressure was measured by a 'Dynisco' pressure transducer attached to the base drainage system. The response of the pore-pressure measuring system with a saturated, sealed specimen in place was checked by applying a sudden increase in cell pressure. The time for 95% equalisation of the pore-pressure was about 1 second.

Continuous records of pore-pressure, axial load and strain variations were made (to a time base) on an ultra-violet recorder. At the same time axial load and strain were cross-plotted directly on an X-Y pen recorder.

### SPECIMEN PREPARATION

The soil used in these studies was a commercially prepared clay, mainly halloysite. Its index properties were: liquid limit, 62%; plastic limit 36%. The specific gravity was 2.60.

The clay was prepared by mixing it to a slurry, using a circulating pump, at a water content of 115%.

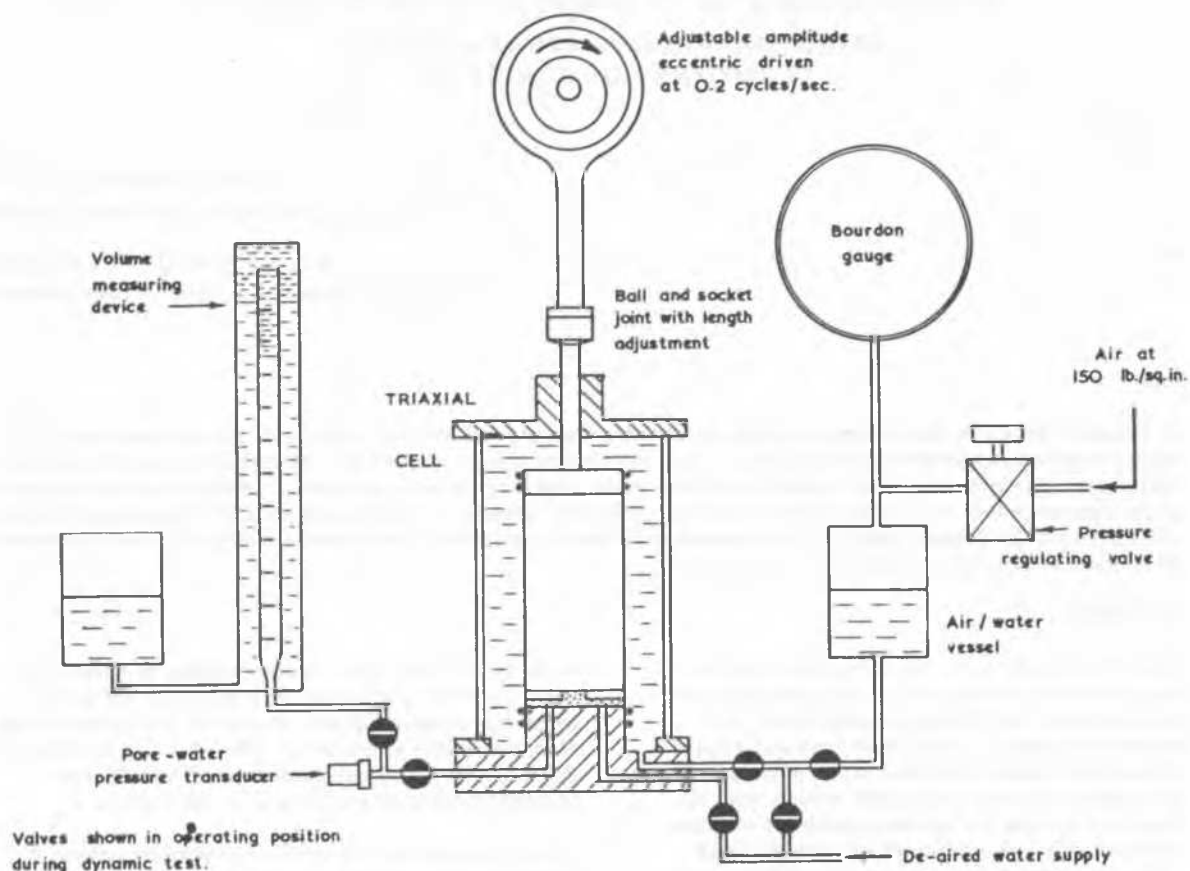


Figure 1: Diagram of Apparatus

At this consistency it could be drawn into a large (10" diameter) oedometer under vacuum. Air entrained during mixing was removed from the slurry by the vacuum as it entered the oedometer. After the clay was consolidated under a vertical stress of 12 p. s. i., 3" diameter  $6\frac{1}{2}$ " long samples were cut and sealed in thin walled brass sampling tubes. These were stored in a constant temperature water bath until required for testing.

Prior to testing, the samples were trimmed to 6" length and weighed. (The excess was used to determine the initial water content.) The specimens were extruded from the sample tubes onto the base pedestal of the triaxial cell and the side drains placed. Before sealing, the specimens were flooded with de-aired water to remove air bubbles remaining under the rubber membrane. The cell was filled with de-aired water and, to ensure complete saturation of the specimen and pore pressure system, the cell pressure was held at 125 lb/sq. in. for 24 hours before permitting drainage. The fully saturated specimens were then consolidated in the triaxial cell to the required maximum consolidation pressure. Consolidation was not truly isotropic as the load

piston was necessarily attached to the top platen which reduced the vertical effective stress by 6% of the cell pressure.

Burette measurements of the total volume change of the specimen during consolidation and swelling, needed to determine area correction, proved unreliable due to the flooding technique used to ensure saturation but this was partly overcome by consolidation in several stages. The change in area was determined from the overall change in weight of the specimen and the axial deformation recorded during consolidation.

All overconsolidated samples were initially consolidated to 64 p. s. i. effective stress then allowed to swell to give overconsolidation ratios of 2, 4, 8, and 16. When volume change had ceased after consolidation or swelling the specimens were kept at equilibrium for 12 hours before testing. The relationship between water content and consolidation stress is shown in Figure 2.

## DYNAMIC CYCLIC STRAIN TESTS ON A CLAY

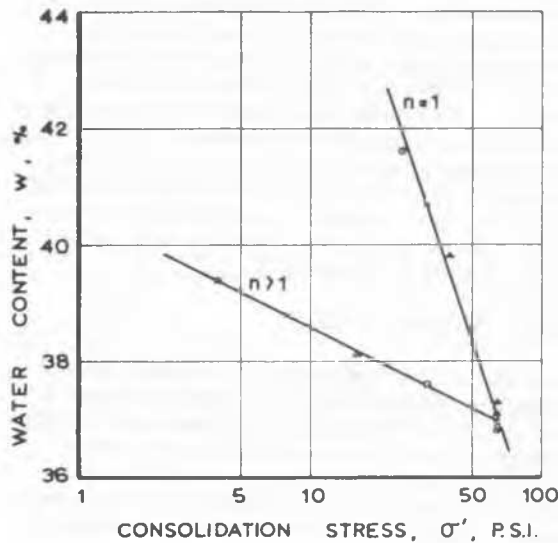


Figure 2: Test Water Contents

### TESTING PROCEDURE

When the cell was aligned the loading rod was connected to the eccentric at the ball and socket joint with special care being taken not to disturb the specimen. As previous investigation (Taylor and Hughes, 1965) had shown that the effect of frequency was small, a frequency of 0.2 c. p. s. was chosen to allow full dynamic pore-pressures to be recorded and to ensure that fluctuation in cell pressure due to load rod movement was negligible.

Pore-pressure, axial load and strain were recorded for 100 applied strain cycles of constant amplitude and the directly plotted load-strain curves were recorded for selected cycles.

After each dynamic test the triaxial cell was transferred to a conventional test machine where the strength characteristics of the specimen were found by loading to failure at a constant strain rate of 1% per minute.

A typical dynamic stress path: shear stress,

$$\tau = (\sigma_1 - \sigma_3)/2$$

plotted against mean effective principal stress,

$$\sigma'_0 = (\sigma_1 + \sigma_2 + \sigma_3)/3$$

is shown in Figure 3. The corresponding dynamic stress-strain curves for the same test are shown in Figure 7(c).

### CHANGE IN EFFECTIVE STRESS WITH CYCLIC STRAIN

In static tests, for example those described by Henkel (1960), it can be noted that the change in resulting from application of a small positive or negative

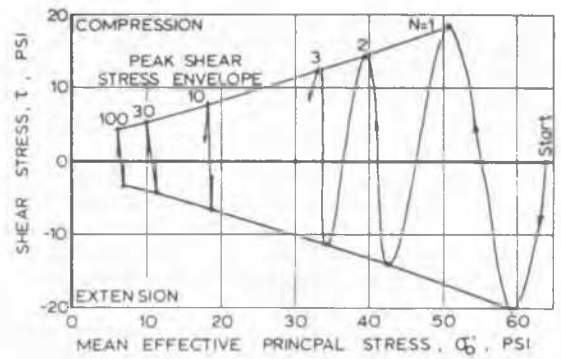


Figure 3: Dynamic Stress Path

deviator stress to isotropically consolidated clay is such that the mean effective principal stress remains constant for small strains.

A small change in mean effective stress is comprised as follows:-

$$\begin{aligned} \delta \sigma'_0 &= \frac{1}{3} \delta (\sigma'_1 + \sigma'_2 + \sigma'_3) \\ &= \frac{1}{3} \delta [(\sigma'_1 - \sigma'_3) + 3(\sigma'_3 - u)] \\ &= \frac{1}{3} \delta (\sigma'_1 - \sigma'_3) + \delta \sigma'_3 - \delta u \end{aligned}$$

When the cell pressure is constant,

$$\delta \sigma'_3 = 0$$

Therefore

$$\delta \sigma'_0 = \frac{1}{3} \delta (\sigma'_1 - \sigma'_3) - \delta u$$

It was clear from the continuous (time base) records of pore-pressure and axial load during dynamic tests that their cyclic fluctuations were similar in form, in phase with each other, and that the magnitude of the pore-pressure fluctuation was close to one third that of the deviator stress. This indicated, as can be seen from the above derivation, that there was little cyclic fluctuation in the mean effective principal stress. For this reason  $\sigma'_0$  rather than pore-pressure, has been adopted as a fundamental parameter and it is suggested that change in  $\sigma'_0$  (at constant void ratio) provides a measure of alteration of the soil micro-structure.

The relationship between mean effective stress and number of cycles,  $N$ , is conveniently shown by plotting  $\sigma'_0$  against  $\log (N+1)$ . Such curves for variations of strain amplitude, maximum consolidation stress, and overconsolidation ratio can be compared in Figure 4 (a), (b), and (c), respectively.

Cyclic strain on normally consolidated clay causes  $\sigma'_0$  to reduce at a decreasing rate from its initial equilibrium value. No lower dynamic equilibrium was reached in 100 cycles although the

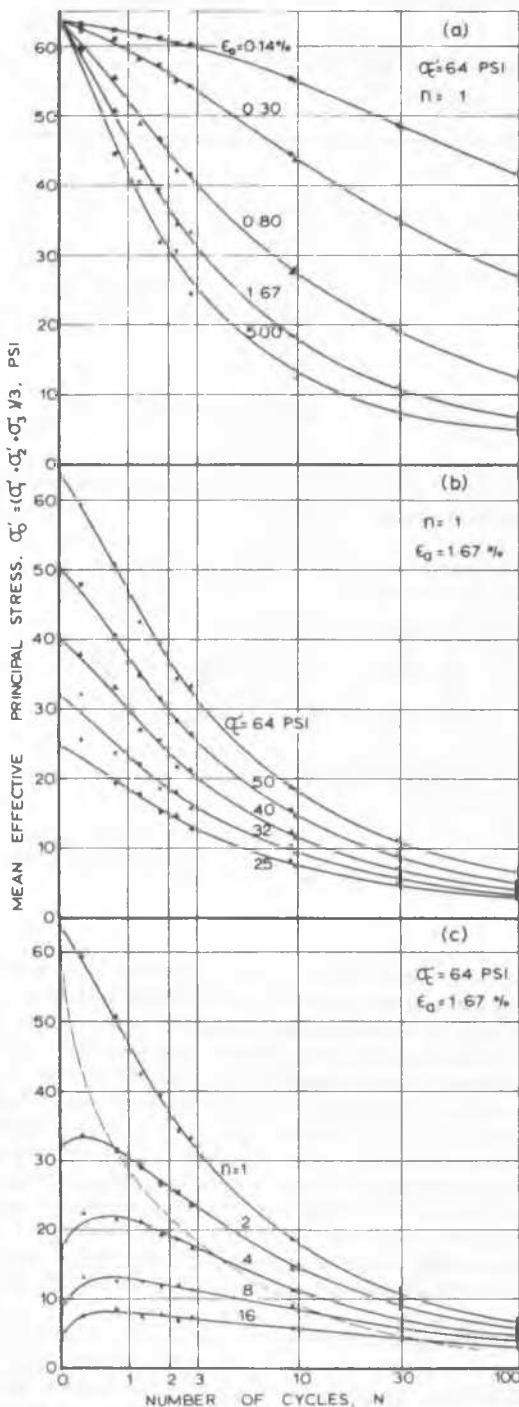


Figure 4: Decrease in Mean Effective Stress during Dynamic Test, with Variation of (a) Strain Amplitude, (b) Consolidation Stress and (c) Over-Consolidation Ratio.

rate of decrease had become very small for higher strain amplitudes. The initial decrement of mean effective stress per cycle,  $g_0$ , in Figure 6 (c), shows a proportional increase with strain amplitude up to  $\epsilon_a = 0.7\%$  and a more gradual increase thereafter. The initial decrement was proportional to the maximum consolidation pressure,  $\sigma'_c$ . For overconsolidated clays  $\sigma'_c$  increased during the first application of strain to a value higher than its initial equilibrium value and then reduced as before. The initial increase became more marked with increasing overconsolidation ratio,  $n$ .

#### DYNAMIC STRESS PATHS

The results of a typical cyclic strain tests on a normally consolidated clay are shown in Figure 3. In this test it can be seen that the peak shear stress,  $\tau$ , holds a linear relationship with the mean effective principal stress,  $\sigma'_0$ . The peak compressive shear stress envelopes for other strain amplitudes (normally-consolidated samples) are shown in Figure 5 (a), and (b).

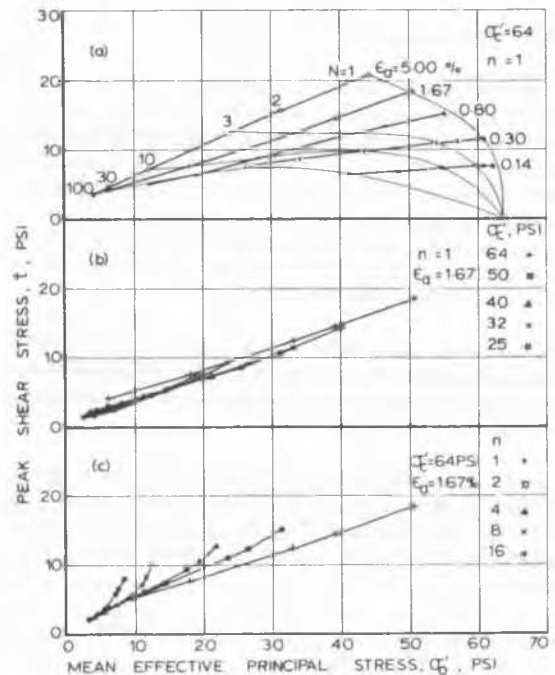


Figure 5: Envelopes of Peak Shear Stress

In each case the envelope was a straight line which could be expressed by  $\tau = a + b\sigma'_0$  which is analogous to the extended Tresca failure criterion. The linearity of the relationship for all values of dynamic strain amplitude indicates that the criterion is valid for conditions other than failure. The parameters  $a$  and  $b$ , shown in Figure 6(a) and (b) may be considered to represent the cohesive and frictional components of developed

# DYNAMIC CYCLIC STRAIN TESTS ON A CLAY

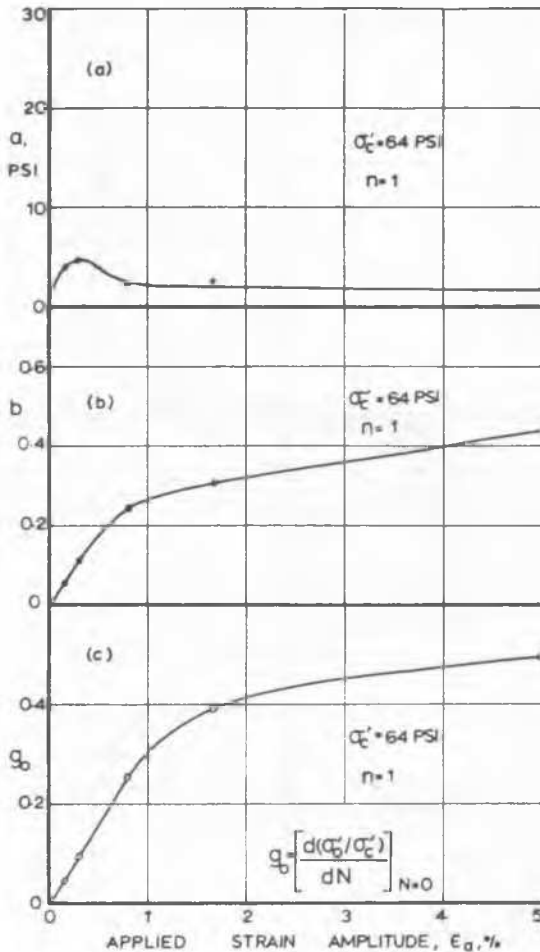


Figure 6: Coefficients  $a$ ,  $b$ , and  $q_0$ .

shear strength. The cohesive component appeared to be developed mainly at small strain amplitudes. The frictional component increased at a decreasing rate with strain amplitude. At a given strain amplitude variation in maximum consolidation pressure caused little change in the peak shear stress envelope and thus little change in  $a$  or  $b$ .

Peak shear stress envelopes for over-consolidated clays with the same maximum consolidation stress are shown in Figure 5(c). The initial peak shear stress was greater than the peak stress of a normally consolidated clay that has been reduced to the same  $\sigma'_c$  by cyclic strain of equal amplitude. After a number of cycles the envelopes converge to the normally consolidated clay stress envelope which thus represents a lower limit of peak shear stress at any strain amplitude.

## STRESS-STRAIN RELATIONSHIPS

Typical dynamic stress-strain curves for the first 3 cycles, the 10th, 30th and 100th cycles are shown

in Figure 7 for three strain amplitudes. These curves have been re-constructed from the directly plotted load-deformation curves by correcting for the area and length of the specimen at the end of consolidation.

Little change in the form of the loop occurs at small strain amplitudes. At large amplitudes significant changes occur. After a few cycles the loop develops an 'S'-shape, with the gradient of the curve at zero strain less than that at peak strain. The gradient (or tangent elastic modulus) increases with increasing strain within a cycle, which is in direct contrast to conventional compression tests on unvibrated clay where the tangent modulus steadily decreases from a maximum at zero strain to zero at failure. The 'S'-shape becomes more marked with increasing number of cycles.

Other investigators have used various parameters to describe the stress-strain loop. Hardin and Black (1968), also Humphries and Wahls (1968) define a shear modulus for torsional vibration as the slope of the line through the ends of the loop. In this paper this parameter will be defined as the average elastic modulus,  $E_a$  = peak shear stress/applied strain amplitude.

Thiers and Seed (1968) define a bilinear 'parallelogram' model with two moduli for dynamic shear box tests. Similar parameters, the minimum and maximum peak elastic moduli,  $E_1$  and  $E_2$ , are here defined as the tangents to the curve at peak strain. A further parameter  $E_0$  is defined as the tangent to the curve at zero strain.

The variation, after 100 cycles, in these four parameters with applied strain amplitude is shown in Figure 8. All increase with decreasing strain amplitude. However for small amplitudes both  $E_0$  and  $E_a$  have values between  $E_1$  and  $E_2$ . At larger amplitudes  $E_0 < E_a < E_1 < E_2$ .

It is to be expected that, in the conventional compression test, performed after each dynamic test, one quarter-cycle of the dynamic stress-strain loop would be repeated. With allowance for experimental error, the results given in Figure 9 show that the same shape is reproduced initially, for samples which have been subjected to dynamic tests at high strain amplitudes. Stress paths to failure are shown for the same tests in Figure 10.

## ENERGY LOSS & DAMPING CHARACTERISTICS

The area of the stress-strain loops which is a measure of the energy loss during cyclic straining, was determined by planimeter to give the specific damping energy,  $D$ , (lb.-in. / (in.)<sup>3</sup>/cycle).

The energy loss for larger amplitudes is initially high but reduces rapidly as the form of the stress-strain curve changes, whereas the energy loss for

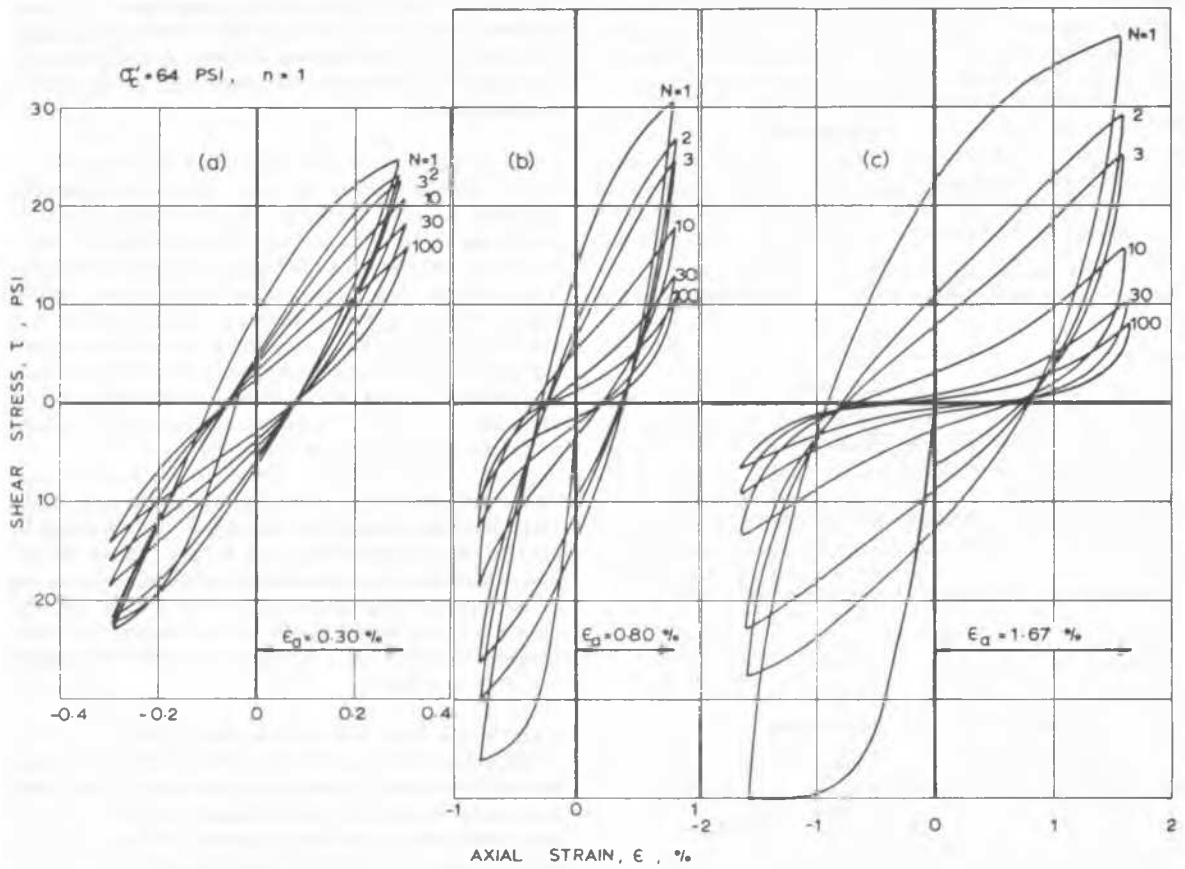


Figure 7: Stress-Strain Loops

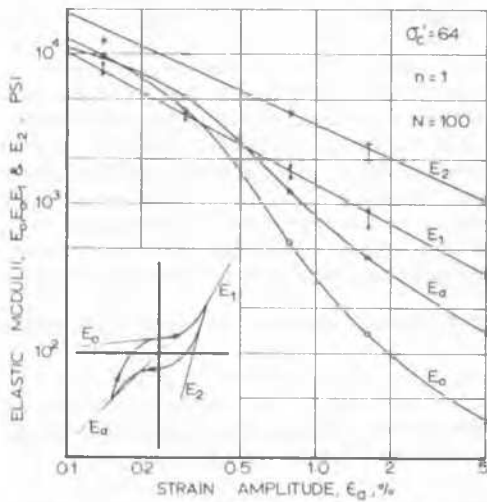


Figure 8: Moduli for 100th Cycle

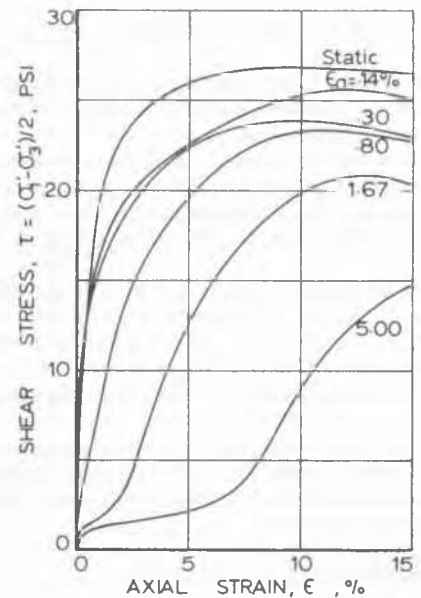


Figure 9: Conventional 'Static' Test Results after Dynamic Tests

## DYNAMIC CYCLIC STRAIN TESTS ON A CLAY

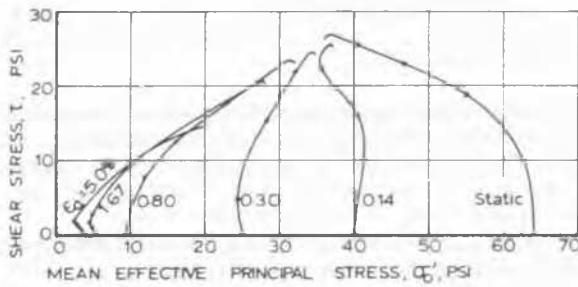


Figure 10: Stress Paths to Failure after Dynamic Tests

small amplitudes is small and relatively constant.

The relationship between specific damping energy and mean effective principal stress is shown in Figure 11 and can be expressed as -

$$D = K (\sigma'_0)^{1.3} \text{ for normally consolidated clays where } K \text{ is a function of the applied strain amplitude.}$$

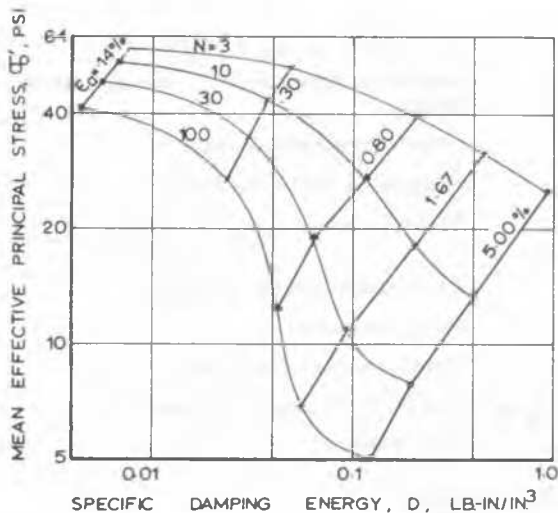


Figure 11: Damping Energy as a Function of Mean Effective Principal Stress

### DISCUSSION

It seems probable that the reduction in mean effective stress observed during cyclic straining is due to a rearrangement of clay particles into "domains" within which the particles are more or less aligned. This more efficient packing results in an increase of pore-water pressure under undrained conditions tending to an equilibrium configuration. (If drainage were allowed, equilibrium would be re-established at a lower void ratio for the same effective stress.)

The reverse curvature, or 'S'-shape of the stress-

strain loop, with the pointed ends tending to be parallel to the axis of stress is of interest. The only materials, other than clays, which behave in this way are some elastomers and polymers (Lazan, 1968, p. 110). 'S'-shaped loops, with the points tending to be parallel to the axis of strain are, of course, observed for most ductile materials, at high strains.

Possibly the earliest published work showing the phenomenon of the 'S'-shape stress-strain loop in soils referred to cyclic torsion tests on unfired ceramic materials (Macey, 1948). More recently, similar but more refined tests made by the British Ceramic Research Association show the same result, and a mechanism has been suggested (Astbury and Moore, 1965) which fits the experimental data extremely well. The mechanism postulated is that the shearing resistance of the clay is derived from numerous elastic elements and viscous elements, and that as elastic strain energy increases, the elastic elements break down and convert to viscous elements. In the steady state condition the viscous elements revert to elastic elements during a later part of the cycle as elastic strain energy decreases. The concept is intriguing, but the authors admit that the model is "not free from physical and indeed, philosophical difficulties of interpretation".

The effect has been noticed in earlier tests at Auckland University (Taylor and Hughes 1965) and has appeared, though without comment, in work done at Berkeley, (Thiers 1966, Figure V.20).

A somewhat similar stress-strain relationship has been observed in dense sands in which liquefaction had been induced by dynamic loading (Seed and Lee, 1966). In that case the increase in resistance to deformation at peak (compression and extension) stress could be attributed to an increase in effective stress (i. e. a decrease in pore-pressure) due to dilation. At zero strain the effective stress reduced to zero, when pore-pressure equalled cell pressure and the resistance to deformation became negligible. This is shown in Figure 12(a).

In the case of the clay, however, the 'S'-shape of the stress-strain curves cannot be explained by dilation. As seen in Figure 12(b) the pore pressure follows the deviator stress, being a maximum at the same time. Expressing the results in terms of the mean effective principal stress  $\sigma'_0$  it is seen that, for the clay, this remains relatively constant throughout the cycle whereas for the sand,  $\sigma'_0$  drops to zero twice during each cycle.

It may be noted from Figure 10 that the stress paths determined for samples, all initially normally consolidated at 64 p. s. i., subjected to dynamic strain, then tested statically, are typical of over-consolidated clays. The dynamic strain has in effect made them over-consolidated but the decrease in effective stress has occurred at constant void ratio and not accompanied by the swelling which occurs when



effective stress is statically reduced.

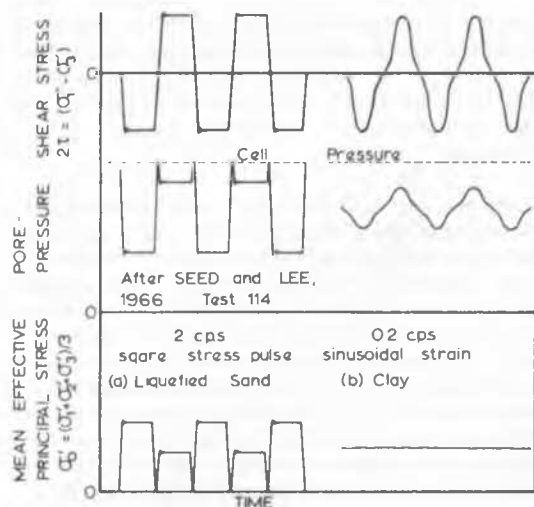


Figure 12: Comparison of Dynamic Tests on Sand and Clay.

## CONCLUSIONS

Despite the fact that this investigation was concerned with a particular clay, some of the conclusions are believed to be valid generally.

1. In strain-controlled dynamic tests on clay (for strains up to 5% for the clay tested) pore pressure change is related to change in principal stresses so that the mean effective stress  $\sigma'_0$  shows negligible cyclic variation.
2. For normally consolidated clay,  $\sigma'_0$  continuously decreases at a reducing rate during cyclic straining, the initial rate of decrease being dependent on strain amplitude.
3. The relationship  $\hat{\tau} = a + b\sigma'_0$  is established for cyclic strain tests on normally consolidated clay. For the clay tested this applied up to a strain amplitude of 5%; the cohesive component,  $a$ , reached a maximum at a strain amplitude of 0.4% while the frictional component increased (but at a decreasing rate) with strain amplitude.
4. For over-consolidated clay,  $\sigma'_0$  increases during the first strain cycle then decreases. The initial increase is greater with higher over-consolidation ratio.
5. For over-consolidated clay, peak shear stresses initially lie outside the envelope found for the normally consolidated clay at the same strain amplitude, but converge towards this envelope with increasing number of strain cycles.
6. Cyclic strain causes a loss in strength, as measured in a conventional test to failure and (for strain in excess of  $\frac{1}{2}\%$  for the clay tested) a reduct-

ion of initial tangent modulus.

## ACKNOWLEDGEMENTS

The experimental work described was performed at the University of Auckland by the second author (D. R. Bacchus) under the supervision of the first (P. W. Taylor) and was considerably facilitated by the support of the N. Z. University Grants Committee. The assistance of a Duke of Edinburgh Scholarship is gratefully acknowledged.

## NOTATION

- |                                   |   |
|-----------------------------------|---|
| $a, b$                            | Coefficients of equation $\hat{\tau} = a + b\sigma'_0$ for peak stress envelope.              |
| $D$                               | Specific damping energy (lb-in/in <sup>3</sup> /cycle).                                       |
| $E_a$                             | Average elastic modulus = $\hat{\tau}/\epsilon_a$   |
| $E_0$                             | Zero strain elastic modulus, tangent to stress-strain loop at zero strain.                    |
| $E_1, E_2$                        | Maximum and minimum peak strain elastic moduli, tangent to stress-strain loop at peak strain. |
| $\sigma'_0$                       | Mean effective principal stress = $\frac{1}{3}(\sigma'_1 + \sigma'_2 + \sigma'_3)$            |
| $\sigma'_c$                       | Maximum value of $\sigma'_0$ during consolidation.  |
| $n$                               | Over-consolidation ratio  |
| $N$                               | Number of strain cycles   |
| $\tau$                            | Shear Stress = $\frac{1}{2}(\sigma'_1 - \sigma'_3)$   |
| $\hat{\tau}$                      | Peak shear stress in a cycle  |
| $u$                               | Pore-pressure   |
| $\epsilon_a$                      | Applied strain amplitude  |
| $\sigma'_1, \sigma'_2, \sigma'_3$ | Effective principal stresses  |
| $\sigma'_3$                       | Cell pressure   |

## REFERENCES

- Astbury, N. F. and Moore, F. (1965), "Torsional Hysteresis in Plastic Clay and its Interpretation", A. S. T. M. Materials Research and Standards, Vol. 5, No. 4, pp. 178-183.
- Hardin, B. O. and Black, W. L. (1968), "Vibration Modulus of Normally Consolidated Clay", Journal A. S. C. E., Vol. 94, No. S. M. 2, pp. 353-369.
- Henkel, D. J. (1960), "The Relationship between the Effective Stresses and Water content in Saturated Clays", Géotechnique, Vol. 10, No. 2, pp. 41.
- Humphries, W. K. and Wahls, H. E. (1968), "Stress History Effects on Dynamic Modulus of Clay", Journal A. S. C. E., Vol. 94, No. S. M. 2, pp. 371-389.

#### **DYNAMIC CYCLIC STRAIN TESTS ON A CLAY**

**Lazan, B. J. (1968), "Damping of Materials and Members in Structural Mechanics", - Pergamon Press.**

**Macey, H. H. (1948), "Experiments on Plasticity - Some Experiments with Alternating Stresses", Trans. Brit. Ceramic Soc., Vol. 47, pp. 183 and 259.**

**Seed, H. B. and Lee, K. L. (1966), "Liquefaction of Saturated Sands During Cyclic Loading", Journal A. S. C. E., Vol. 92, No. S. M. 6, pp. 105-134.**

**Taylor, P. W. and Hughes, J. M. O. (1965), "Dynamic Properties of Foundation Subsoils as determined from Laboratory Tests", Proc. 3rd World Conf. Earthquake Eng., Vol. I, pp. 196-211.**

**Thiers, G. R. (1966), "The Behaviour of saturated clay under Seismic Loading Conditions", Ph. D. Thesis, University of California, Berkeley, California.**

**Thiers, G. R. and Seed, H. B. (1968), "Cyclic Stress-Strain Characteristics of Clay", Journal A. S. C. E., Vol. 94, No. S. M. 2, pp. 555-569.**